DMD Fast Forward. Published on October 20, 2008 as doi:10.1124/dmd.108.023408

DMD #23408

Structural Modulation of Oxidative Metabolism in Design of Improved Benzothiophene Selective Estrogen Receptor Modulators (SERMs)

*Zhihui Qin, Irida Kastrati, Rezene T. Ashgodom, Daniel D. Lantvit, Cassia R. Overk, Yongsoo Choi, Richard B. van Breemen, Judy L. Bolton, and Gregory R. J. Thatcher**

Department of Medicinal Chemistry and Pharmacognosy
College of Pharmacy
University of Illinois at Chicago
833 S. Wood St., M/C 781, Chicago, IL 60612-7231

Running Title: Modulation of oxidative metabolism of benzothiophene SERMs.

Dr. Greg. Thatcher
Department of Medicinal Chemistry and Pharmacognosy
College of Pharmacy, University of Illinois at Chicago
833 South Wood St., M/C 781, Chicago, IL 60612
Phone: (312)-355-5282
FAX: (312)-996-7107
Email: thatcher@uic.edu

PAGES:	38
TABLES:	0
FIGURES:	8
REFERENCES:	38

WORDS: (excluding in text reference citations)

Abstract	234
Introduction	615
Discussion	1250

Abbreviations: Arz, arzoxifene; BDE, bond dissociation energy; DFT, Density Functional Theory; DMA, desmethylated arzoxifene; DMA-SG, glutathionyl-desmethylated arzoxifene; DMSO, dimethyl sulfoxide; E2, estradiol; ER, estrogen receptor; GSH, glutathione; LC-MS-MS, liquid chromatography-tandem mass spectrometry; PCA, Principal Components Analysis; Ral, raloxifene; SERM, selective estrogen receptor modulator; UDPGA, uridine-5'-diphosphoglucuronic acid.

Abstract. Raloxifene and arzoxifene are benzothiophene selective estrogen receptor modulators (SERMs) of clinical use in postmenopausal osteoporosis and treatment of breast cancer and potentially in hormone replacement therapy (HRT). The benefits of arzoxifene are attributed to improved bioavailability over raloxifene, whereas the arzoxifene metabolite, desmethylarzoxifene (DMA) is a more potent antiestrogen. As polyaromatic phenolics, benzothiophene SERMs undergo oxidative metabolism to electrophilic quinoids. The long-term clinical use of SERMs demands increased understanding of correlations between structure and toxicity; metabolism being a key component. An homologous series of 4'-X-4'-desmethoxyarzoxifene (X-DMA) derivatives was developed and metabolism studied in liver and intestinal microsomes. Formation of glutathione (GSH) conjugates was assayed in rat liver microsomes and novel adducts were characterized by LC-MS-MS. Formation of glucuronide conjugates was assayed in human intestine and liver microsomes, demonstrating formation of glucuronides ranging from 5% to 100% for the benzothiophene SERMs: this trend was inversely correlated with the loss of parent SERM in rat liver microsomal incubations. Molecular orbital calculations generated thermodynamic parameters for oxidation which correlated with Hammett substituent constants, however, metabolism in liver microsomes correlated with a combination of both Hammett and Hansch lipophilicity parameters. The results demonstrate a rich oxidative chemistry for the benzothiophene SERMs, the amplitude of which can be powerfully modulated, in a predictable manner, by structural tuning of the 4'-substituent. The predicted extensive metabolism of DMA was confirmed in vivo and compared to the relatively stable arzoxifene and F-DMA.

Introduction

Hormone replacement therapy (HRT) remains a cornerstone of contemporary women's healthcare, despite recent outcomes from the Women's Health Initiative clinical trials that illustrated the elevated risks of breast cancer and stroke associated with HRT (Rossouw et al., 2002; Beral, 2003). These trials also confirmed the benefits of HRT including reductions in the incidence of colon cancer, osteoporotic fractures, and postmenopausal symptoms, highlighting the need for new HRT agents with minimized risk factors. The central role of estrogens in female reproduction and beneficial effects on the skeletal, cardiovascular, and central nervous systems, results in the clinical observations in postmenopausal women of higher incidence of osteoporotic fractures, coronary heart disease, hot flashes and lower reported quality of life. Selective estrogen receptor modulators (SERMs) that elicit the beneficial effects of estrogens, but either do not elicit or antagonize estrogens' detrimental effects hold promise as HRT agents.

SERMs as a class of therapeutic agents are thought to evoke their actions through selective agonist and antagonist action at the estrogen receptor (ER). An ideal SERM would be tissue selective having pro-estrogenic or agonist activity in bone, the cardiovascular system, and the CNS, whilst exerting antagonist or anti-estrogenic activity in the breast and uterus (Conzen, 2003). Tamoxifen is the prototype SERM, and is in use for the treatment and prevention of hormone-dependent breast cancer; raloxifene (Evista ®) is a benzothiophene SERM with improved tissue selectivity, approved for the treatment and prevention of postmenopausal osteoporosis (Fig. 1) (Delmas et al., 1997). The "Study of Tamoxifen and Raloxifene" (STAR trial) compared the safety and effectiveness of these two agents for the prevention of breast cancer in postmenopausal women (Kelminski, 2002). The STAR trial recently reported out that raloxifene is as effective as tamoxifen in reducing the risk of invasive breast cancer and has a lower risk of thromboembolic

events (Vogel et al., 2006). In search of an ideal SERM, newer generations of SERMs, such as arzoxifene, acolbifene and lasofoxifene have been developed (Fig. 1). Arzoxifene is a next generation benzothiophene SERM reported to have better bioavailability than raloxifene, resulting in a more favorable therapeutic and safety profile.

ER ligands, including SERMs, are generally polyaromatic phenols susceptible to oxidative metabolism. A contribution to the well-known carcinogenic potential of tamoxifen has been proposed to result from oxidative metabolism to reactive metabolites including quinones (van Leeuwen et al., 1994). The detection of DNA adducts in women on tamoxifen therapy supports a genotoxic pathway resulting from oxidative bioactivation (Shibutani et al., 2000). The facile oxidation of raloxifene, DMA (desmethylarzoxifene), and acolbifene to electrophilic quinones has also been reported (Yu et al., 2004; Liu et al., 2005a; Liu et al., 2005b).

It has long been recognized that a contribution to the carcinogenic actions of endogenous estrogens results from chemical mechanisms (Yager and Liehr, 1996), including oxidative metabolism to catechol and quinoid reactive metabolites (Bolton et al., 2000). The development of fluoroestradiol by Liehr was aimed at blocking the aryl carbons susceptible to metabolic hydroxylation and further oxidation to an *o*-quinone (Liehr, 1983; Liehr, 1984). Fluoroestradiols showed reduced carcinogenic potential relative to the endogenous estrogens, but metabolic defluorination was reported, possibly hindering the proposed potential use as new HRT agents. In a similar vein, 4'-fluoro-substitution was employed in, F-DMA, an analog of arzoxifene, to improve metabolic stability, attenuate toxicity via quinoid formation, whilst minimizing the impact upon ER-mediated biological activity (Liu et al., 2005a; Liu et al., 2006). To elaborate a more complete correlation of structure with activity and toxicity, an extended family of 4'-substituted-4'-desmethoxyarzoxifene derivatives (X-DMA SERMs) has been developed. The ER-dependent

and ER-independent activity of this family has recently been reported, along with structure correlations with oxidative reactivity (Overk et al., 2007; Qin et al., 2007; Yu et al., 2007). In this paper, structure correlations for this family are extended to oxidative metabolism and glucuronidation in vitro and in vivo. Benzothiophenes SERMs are an important family of clinical agents, the use of which in therapy is likely to expand in the future, therefore a full understanding of the relationship of structure to activity, reactivity, and metabolism is essential.

Materials and Methods

Materials. Optima grade acetonitrile and methanol were purchased from Fisher Scientific (Itasca, IL), other chemicals were purchased from Aldrich Chemical (Milwaukee, WI). Alamethicin, UDPGA were purchased from Sigma (St. Louis, MO). Pooled human intestine microsomes and pooled human liver microsomes were obtained from In Vitro Technologies (Baltomore, Maryland). Rat liver microsomes were prepared according to an existing procedure (Yu et al., 2007). All the SERM molecules used in this study were synthesized as reported previously (Liu et al., 2005a; Qin et al., 2007).

Instrumentation. LC-MS-MS was carried out using an Agilent (Palo Alto, CA) ion trap mass spectrometer equipped with a model 1100 HPLC system and electrospray ionization source. The analytical HPLC analysis of the incubations of SERMs with microsomes was performed using an Agilent Eclipse XDB-C18 column (4.6×250 mm, 5 μm) with UV absorbance detection at 316 nm and MS-MS analysis. The mobile phase consisted of a linear gradient from 10% acetonitrile in water containing 10% methanol and 0.1% formic acid at 1 ml/min as follows: 10 - 30% acetonitrile over 20 min, 20 min gradient from 30 - 60% acetonitrile, and then 60 - 90% acetonitrile over 5 min.

Calculations. Geometry optimizations were performed at the (U)B3LYP/6-31+G(d) level using Gaussian 03 (Gaussian Inc., Wallingford, CT). These structures were fully characterized as energy minima by harmonic vibrational frequency analysis and confirmed to have adequate convergence and zero imaginary vibrational frequencies. For the radical species, spin determinant calculations were evaluated to check for spin contamination. Thermodynamic parameters obtained using these Density Functional Theory (DFT) calculations were used to obtain O-H bond dissociation energies (BDE). VolSurf (Molecular Discovery Ltd., UK) as implemented in Sybyl (Tripos, St Louis MI) was used to calculate CYP3A4 metabolic stability.

Bioactivation of SERMs by Rat Liver Microsome. A solution containing the SERM substrate (10 μM), rat liver microsomes (1mg/ml), GSH (500 μM) and NADPH (1mM) in 50mM phosphate buffer (pH 7.4, 500 μl total volume) was incubated for 30 min at 37°C. For control incubations, NADPH or GSH were omitted. The reactions were terminated by chilling in an ice bath followed by the addition of a mixture of methanol/acetonitrile (100 μl, 1:1 v/v) and perchloric acid (50 μl/ml). The reaction mixtures were centrifuged at 13000 rpm for 10min, aliquots (80 μl) of supernatant were analyzed using LC-MS with the HPLC method described above.

Microsomal Stabilities in Rat Liver Microsome. A solution containing the SERM substrate (1 μM), rat liver microsomes (0.5mg/ml), NADPH (1mM) in 50mM phosphate buffer (pH 7.4, 300 μl total volume) was incubated for 30 min at 37°C. The reactions were terminated by chilling in an ice bath followed by the addition of a mixture of methanol/acetonitrile (300 μl, 1:1 v/v) containing perchloric acid (50 μl/ml) and internal standard (azido raloxifene or raloxifene; 1 μM). The reaction mixtures were centrifuged at 13000 rpm for 10 min, aliquots (100 μl) of supernatant were analyzed using LC-MS with the HPLC method described above. For control incubations, a mixture of methanol/acetonitrile (300 μl, 1:1 v/v), aqueous perchloric acid (50

μl/ml) and internal standard (1 μM) was added to a solution containing the SERM substrate (1 μM) and rat liver microsomes (0.5mg/ml), NADPH was then added (as above) to give a total volume of 300 μl. The control mixture was centrifuged at 13000 rpm for 10 min, aliquots (100 μl) of supernatant were analyzed using LC-MS with the HPLC method described above. Azido raloxifene was used as internal standard for quantification of all SERMs except $MeSO_2$-DMA and DMA, where Ral was used as an internal standard, because retention times of azido raloxifene, $MeSO_2$-DMA and DMA were too similar for reliable quantification.

Glucuronidation in Human Liver and Human Intestine Microsomes. A solution containing the SERM substrate (30 μM), human liver microsomes or human intestine microsomes (0.5mg/ml), alamethicin (50 μg/ml), $MgCl_2$ (8 mM) and UDPGA (1mM) in 50mM phosphate buffer (pH 7.4, 300 μl total volume) was incubated for 30 min at 37°C. The reactions were terminated by chilling in an ice bath followed by the addition of a mixture of methanol/acetonitrile (300 μl, 1:1 v/v) and internal standard (30 μM). The reaction mixtures were centrifuged at 13000 rpm for 10 min, aliquots (100 μl) of supernatant were analyzed using LC-MS with the HPLC method described above. For control incubations, a mixture of methanol/acetonitrile (300 μl, 1:1 v/v), perchloric acid (50 μl/ml) and internal standard (30 μM) was added to a solution containing the SERM substrate (30 μM) and human liver microsomes or human intestine microsomes (0.5mg/ml). Similar to the 30min incubation, the same amount of UDPGA, alamethicin, $MgCl_2$ were then added. The control mixture was also centrifuged at 13000 rpm for 10 min, aliquots (100 μl) of supernatant were analyzed using LC-MS with the HPLC method described above.

In vivo plasma metabolite quantitation. Several biomarkers were studied in female juvenile Sprague-Dawley rats as previously described (Overk et al., 2007), in experiments approved by the UIC Animal Care and Use Committee Guide for the Care and Use in accordance

with the Guide for the Care and Use of Laboratory Animals as adopted and promulgated by the NIH. In brief, animals received at 12 d of age from Harlan (Indianapolis, IN) were acclimatized for 1 week with access to water and rat chow ad libitum. Animals received daily either Arz, DMA, or F-DMA (sc; 10 mg/kg), with or without E_2 (E_2 benzoate; sc; 0.1 mg/kg), for 3 days. 24 h after the last injection, animals were sacrificed by bottle CO_2 and blood collected. Blood (1 ml) was placed on ice, centrifuged, and serum stored at -80□C. Aliquots (60 µl) of pooled sera were diluted in acetonitrile (180 µl) and centrifuged to precipitate proteins at 10,000g and 4□C for 5 min; supernatant was dried in vacuo and dissolved in methanol (50 %; 90 µl) for analysis. LC-MS analysis was carried out using separation by a Shimadzu LC-10D VP HPLC system on a Waters XTerra MS C_{18} column (2.1 mm x 100 mm, 3.5 µ) using an 18 min linear gradient (50 to 80% MeOH in 0.1% aq. formic acid) followed by 1 min isochratic 80% MeOH. Positive ion electrospray MS-MS was performed on Applied Biosystems API 4000 triple quad spectrometer using collision-induced dissociation and multiple reaction monitoring (MRM): capillary voltage 4500 V; ion source 450□C; collision energy 41 V; dwell time 350 ms/MRM transition. MRM transitions of m/z 462 to 112, 464 to 112, 476 to 112, 474 to 112 were used for DMA, F-DMA, Arz and Ral, respectively.

Results

Calculated Oxidative Lability of X-DMA SERMs. DMA and NH_2-DMA can form a diquinone methide and a quinone-imine methide, respectively, whereas all other X-DMA SERMs are blocked from oxidation beyond the phenoxyl radical (Fig. 2). Computer calculations were performed on the substituted 2-phenylbenzothiophene core to allow a higher level of calculation. The calculated 1st electron oxidation energies (or O-H bond dissociation energy; BDE) for DMA

DMD Fast Forward. Published on October 20, 2008 as DOI: 10.1124/dmd.108.023408
This article has not been copyedited and formatted. The final version may differ from this version.

and NH_2-DMA were very similar and at the low level expected for good phenolic antioxidants: 73-74 kcal/mol. However, the 2nd electron oxidation was substantially lower in energy for DMA and substantially higher for NH_2-DMA (Fig. 2A). The expectation from these calculations is that DMA will not form a phenoxyl radical, but will undergo direct 2 electron oxidation to the quinone; whereas, NH_2-DMA will form a phenoxyl (or semiquinone-imine) radical as product, or as a discrete intermediate in oxidation to the quinone-imine.

Fig. 2

For the entire X-DMA series, the free energy and BDE for OH bond homolysis was calculated and correlated with Hammett substituent parameters, generating an excellent correlation with σ_p and yielding a ρ value of 1.9, reflecting the strong stabilization of the electron deficient phenoxyl radical by more electron donating 4'-substituents, despite the remoteness of this substituent from the radical center (Fig. 2B).

Identification of Metabolites of X-DMA SERMs and Raloxifene in Rat Liver Microsomes. Incubations of SERMs in liver microsomes from rats treated with dexamethasone to induce CYP450 3A4 were performed for 30 min in the presence of NADPH and GSH. We have previously reported the formation of GSH conjugates under such conditions for both raloxifene (Ral) and DMA (Yu et al., 2004; Liu et al., 2005a). Accordingly, raloxifene was readily oxidized to a diquinone methide (DiQM) which was trapped by GSH to give a mono-GSH conjugate as the major metabolite (DiQMGSH), with subsequent peptide cleavage yielding DiQMCys-Gly and DiQMCys (Fig. 3). As previously reported, a minor flux of oxidative bioactivation leads to the benzothiophene *o*-quinone (*o*-Q), which is trapped by GSH to yield *o*-QGSH. DMA was also readily oxidized to a diquinone methide, leading to a series of conjugates (DiQMGSH), several of which we have previously rigorously identified (Liu et al., 2005a). *N*-dealkylation, a well-known

CYP450 catalyzed reaction for SERMs was also observed for DMA in these incubations and characterized by LC-MS-MS (Figs 3, 4B).

Figs 3, 4

The formation of a quinone-imine from NH_2-DMA is theoretically possible, but molecular orbital calculations indicated that this reactive metabolite is less energetically accessible than the corresponding diquinone methide (*vide supra*). A GSH conjugate was observed (Quinoneimine-GSH; Fig. 3), but this was a minor metabolite. In the rat liver microsome incubations, NH_2-DMA produced an *N*-dealkylation and a dehydrogenation product. Interrogation by LC-MS-MS analysis of the metabolites formed from NH_2-DMA yielded a surprise in the observation of a GSH conjugate derived from displacement at the 3-position of the benzothiophene ring, in simile with previous observations on DMA (Figs 3, 4A) (Liu et al., 2005a). The proposed mechanism for formation of this conjugate is a Michael-type addition at the 3-position of the quinone imine methide, followed by collapse of the intermediate to expel the 3-phenoxy leaving group. $MeSO_2$-DMA was not expected to be susceptible to bioactivation, because diquinone methide formation is blocked and the electron-withdrawing substituent diminishes the potential for 1 electron oxidation. Nevertheless, a GSH conjugated metabolite was observed and characterized by LC-MS-MS as the di-GSH adduct of the *o*-quinone (*o*-quinoneDiGSH; Figs 3, 4C). Similarly, F-DMA and Br-DMA were both expected not to be oxidatively labile. In this case, in accord with expectations, little metabolism of F-DMA and Br-DMA was observed in rat liver microsomes (Fig. 5), and attempts were not made to identify the very minor amounts of these metabolites.

Fig. 5

Arzoxifene (Arz) may function in large part as a DMA-prodrug, but in rat liver microsomes, after incubation of Arz for 30 min, only minor demethylation was observed. Interestingly, in these

experiments oxidation of H-DMA gave a higher yield of DMA than Arz, showing that H-DMA can function as a DMA prodrug (Fig. 5). Oxidation of Arz to an *o*-quinone was shown by the detection and characterization by LC-MS-MS of a GSH adduct (Fig. 5). In several microsomal incubations, minor products were observed and identified by LC-MS as probable products of ring hydroxylation mediated by CYP450.

Quantification of Metabolism in Rat Liver Microsomes. The quantities of SERMs required in experiments designed to identify metabolites (10 μM) is greater than the pharmacologically relevant concentrations of SERMs, therefore, the extent of metabolism of the X-DMA SERMs in induced-rat liver microsomes was quantified at tenfold lower concentration (Fig. 6). Under these conditions, the parent SERM remaining after 30 min incubation was quantified by HPLC/UV. Authentic standards assayed in identical reaction media were used to provide calibration. The quinone forming SERMs, Ral, DMA, and NH_2-DMA, were highly metabolized under these conditions; only 10-22% parent drug remained. Interestingly, H-DMA was also metabolically labile under these conditions, compatible with the oxidation of H-DMA to the oxidatively active DMA, consistent with observations on H-DMA described above (Fig. 5). In contrast, F-DMA and Br-DMA were observed substantially intact in rat liver microsome incubations, compatible with the observation of only minor metabolites at higher concentrations of these X-SERMs.

The only X-SERM for which the disappearance of parent molecule at lower concentration (Fig. 6) appeared strongly at odds with the identification of metabolites at higher concentrations (Fig. 5) was $MeSO_2$-DMA. Therefore, the metabolic depletion of $MeSO_2$-DMA was further examined by using alternative extraction protocols to rule against this observation being caused by inefficient extraction and recovery. However, the observed substantial loss of parent $MeSO_2$-

DMA did not vary when different protocols were employed. A second route to examine the apparent anomaly of $MeSO_2$-DMA was the study of this X-DMA SERM in P450 supersomes. Metabolites were identified in incubations with human P450 3A4 supersomes: the action of CYP450 3A4 gave an *o*-quinone monoGSH conjugate (*o*-QGSH) of $MeSO_2$-DMA, in addition to substantial *N*-dealkylation, the latter occurring both in the absence and presence of GSH (data not shown).

Fig. 6

Quantification of phase II metabolism in human intestinal and liver microsomes. In order to assess phase II conjugative metabolism and draw comparisons with data generated in rat liver microsomes, human microsomal liver and small intestine fractions were studied, both obtained from commercial sources. In the presence of UDPGA, glucuronide conjugates were anticipated. Previously, in cryopreserved rat hepatocyte incubations, two DMA glucuronide conjugates were observed which fragmented to produce the protonated aglycon formed from cleavage of the glycosidic bond (MH^+-176) (Liu et al., 2006). In incubations of F-DMA with rat hepatocytes, only one glucuronide conjugate was detected, giving the characteristic fragment (MH^+-176). Therefore, it was expected that SERMs with a 4'-substituent available for conjugation would be more extensively glucuronidated. This expectation was borne out by the observation of almost complete glucuronidation of DMA and to a lesser extent Ral under the assay conditions (Fig. 6B). The available 4'-NH_2 group of NH_2-DMA is also susceptible to conjugation, leading to 50% glucuronide formation in the human microsomes. The observed lower relative glucuronide formation from the other X-DMA SERMs reflected the lack of a 4'-conjugating group, with the two halo-DMA derivatives, Br-DMA and F-DMA, again demonstrating high metabolic stability. Data obtained from human liver microsomes were more variable than from the intestinal

microsomes, but the trends in relative reactivity towards glucuronidation were similar in both systems.

Correlation of metabolic stability with substituent parameters. A primary objective in developing the X-DMA SERMs was correlation of activity and reactivity with the molecular properties induced by the 4'-substituent. The coefficient for correlation of hepatic metabolic lability (using the measurement of % SERM remaining in liver microsomes; Fig. 6A) with redox reactivity (as given by the calculated O-H BDE; Fig. 2) was poor ($R < 0.4$). Good correlations have been reported between substrate binding and substrate lipophilicity for many CYP families (Hansch and Zhang, 1993; Gao and Hansch, 1996; Sarver et al., 1997; Lewis et al., 2004). Accordingly, correlation with ClogP was assayed, yielding a coefficient of correlation for liver metabolism versus ClogP values (Fig. 1) calculated for each of the SERMs studied which was much improved ($R = 0.77$; Fig. 7A). For comparison, it should be noted that the ClogP values calculated for typical substrates of CYP3A4 and CYP2C9 are 3.4 and 3.2, respectively, compared with the uniformly higher ClogP values for the X-DMA SERMs. Consequently, a classical Hansch correlation was performed. It was found that incorporation of the 4'-substituent lipophilicity parameter (π) with substituent electronic effects (using the 4'-substituent Hammett parameter; σ_p) led to an excellent correlation with the experimental data ($R = 0.92$; Fig. 7B) (Hansch et al., 1995). Of interest from this correlation is that the apparently aberrant metabolic lability of $MeSO_2$-DMA (Fig. 6A) is accounted for by the contribution of lipophilicity to CYP-mediated metabolism. This conclusion is compatible with the bell-shaped correlations of substrate binding with lipophilicty which have been reported for CYP isoforms, with preferred substrates being of lower lipophilicity than the X-DMA SERMs. Finally, the correlation of microsomal

glucuronide formation with SERM metabolism demonstrates the importance of the 4'-substituent in conjugative metabolism (Fig. 7C).

Fig. 7

Correlation of metabolic stability with *in silico* stability. Unexpected toxicity and drug-drug interactions have been blamed for large-scale failure of drug candidates, prompting the widespread use of *in silico* pharmacokinetic algorithms. VolSurf is a computational algorithm that produces 2D molecular descriptors from 3D molecular interaction energy grid maps. Most of the 94 molecular descriptors are physicochemical descriptors quantifying size, shape, polarity, hydrophobicity and combinations thereof. In order to predict metabolic stability towards CYP3A4, the developers used QSAR analysis of 1800 compounds from Pharmacia reporting an optimal distance of ~9Å to 18Å separating the aromatic interacting regions of CYP3A4 substrates. This geometric arrangement suggests that the methodology should be applicable to benzothiophene SERMs. Therefore, VolSurf molecular descriptors were generated for the X-DMA series giving 5 different sets of predicted CYP3A4 susceptibility values (derived from each of 5 PCAs). Correlation with observed metabolic lability in induced rat liver microsomes was superior with PCA1 and PCA2 as 2D descriptors, however, in both cases, F-DMA was an outlier (Fig. 7D): PCA1 score $r^2 = 0.29$ (or 0.91 without F-DMA); PCA2 score $r^2 = 0.34$ (or 0.91 without F-DMA). The rationale for this discrepancy may lie with the low level AM1 calculations used in this methodology to derive 3D descriptors, or the overestimation of de-fluorination rates from the training set compounds; however, the fit is sufficiently good to encourage cautious use in SERM development.

Metabolism of X-DMA SERMs in vivo. As part of a comparative study of biological activity of DMA, Arz, and F-DMA in juvenile female rats, metabolism was assessed by

quantification of remaining drug in plasma after 3 days of drug administration (Overk et al., 2007; Yu et al., 2007). Since this animal study was in part designed to assess the estrogenic and antiestrogenic activity of these SERMs, arms were included in which animals were co-administered estradiol as the benzoate (EB). Although the bioavailability component of the juvenile rat study was confined to measurement of remaining unmodified drug, the results provide both a useful correlation with the in vitro measures of drug metabolism, described above, and indicate an unexpected avenue for future study. The observed effect of estradiol co-administration was significantly to attenuate the metabolism of Arz (Fig. 8); this effect which may operate via estrogenic CYP regulation is worthy of further study.

The bioavailability data show extensive metabolic depletion of DMA, contrasted with the relative stability of Arz and F-DMA. In 60 μL of rat plasma in the absence of estradiol, these parent SERMs were measured at levels of 5.5 ng and 5.3 ng, respectively. The absolute bioavailability of Ral in humans is only 2%, argued to result from extensive glucuronidation (Hochner-Celnikier, 1999), which is reported to occur preferentially at the 4'-position in vivo (Kemp et al., 2002). DMA is anticipated to have equally poor bioavailability, which is confirmed in rats by the results shown in figure 8; and is likely also due to extensive glucuronidation on the basis of the comparison of Ral with DMA shown in figure 6.

Fig. 8

Discussion

Previously the comparative metabolism of F-DMA, DMA, and Ral was reported in rat liver microsomes, hepatocytes, and intestinal epithelial cells. The pattern of metabolism, including formation of GSH conjugates, glucuronides, sulfates, and the relative metabolic lability, confirmed

the strong influence of oxidative bioactivation to a diquinone methide (Liu et al., 2005a; Liu et al., 2006). Complementary to the observed patterns of metabolism: depletion of cellular GSH was observed to be attenuated in the presence of F-DMA relative to Ral and DMA; and, DNA damage by F-DMA was negligible in contrast to significant single strand breaks caused by DMA. Given this demonstration of the ability of 4'-modification to modulate reactivity and metabolism, an extended family of 4'-substituted benzothiophene (X-DMA) SERMs was developed and the biological activity reported in cell culture and in the juvenile rat model (Overk et al., 2007; Qin et al., 2007; Yu et al., 2007).

Ral continues to find widespread use in postmenopausal osteoporosis and recent clinical trial data in cancer chemoprevention has permitted use in an additional therapeutic indication(Vogel et al., 2006). The wealth of data on cardiovascular and other secondary endpoints from the largescale RUTH clinical trial (Barrett-Connor et al., 2006), combined with the continued development of Arz as an improved benzothiophene SERM, support the selection of the X-DMA SERMs for detailed structure-activity studies. Furthermore, there remains more to learn about this extended drug class, since we and others have shown that the benzothiophene SERMs possess chemopreventive actions not associated with classical estrogenic activity (Liby et al., 2006; Yu et al., 2007).

The family of Arz analogs selected, possesses a range of structural modifications at the 4'-position which are predicted to strongly influence bioactivation and metabolism, and to provide a wide range of electronic contributions that may be quantified by substituent parameters. The selection of halogen ring substituents is a standard approach to metabolic stabilization in medicinal chemistry. Of special note is the use of fluoro-substituted estrogens to block or inhibit oxidative bioactivation to estrogen *o*-quinones: estrogenic carcinogenicity was absent or reduced in

fluoroestradiols, although these compounds showed comparable estrogenic potency to estradiol (Liehr, 1983). Observations on fluoroestradiols support the hypothesis that toxicity and activity are not intrinsically coupled but are dependent on the chemical structure, which dictates the metabolic profile and characteristics of reactive metabolites. The selection of a 4'-amino substituent is interesting mechanistically, because of the likely formation of a quinone imine oxidative metabolite; and, a methanesulfonyl group was recently employed in a new SERM to limit blood/brain barrier penetration (Hummel et al., 2005).

Metabolism is central to the design of Arz as an evolution from Ral. Orally administered Ral in humans has reported absolute bioavailability of 2% and apparent oral clearance of 44 l/kg/h (Hochner-Celnikier, 1999; Snyder et al., 2000). Intestinal glucuronidation of Ral is reported to be the major contributor to the presystemic clearance of Ral (Kemp et al., 2002). DMA, "the most potent estrogen antagonist described to date that maintains estrogen agonist actions on bone and lipids", was first reported in 1997 (Palkowitz et al., 1997), however, the higher potency of DMA in vitro was lost in vivo because of poor bioavailability again due probably to extensive first pass glucuronidation. Indeed, orally delivered DMA was only equipotent with Ral, despite Ral itself being known to have poor bioavailability and lower potency. The low bioavailability and rapid clearance of DMA is illustrated in this present study by the very low plasma levels in juvenile female rats, whereas both Arz and F-DMA have comparably high bioavailability (Fig. 8). Since 4'-glucurondation is blocked in Arz, this modification of DMA was incorporated simply to increase bioavailability, which appears borne out by published data (Suh et al., 2001; Burke and Walker, 2003). Replacement of the 4'-hydroxyl group of DMA by the 4'-methoxy of Arz reduces first-pass glucuronidation and increases ClogP by approximately 0.6 units (Sato et al., 1998). Arz is observed to be metabolically desmethylated to yield DMA, both in vitro and in clinical samples

after Arz treatment (Buzdar et al., 2003) (Liu et al., 2005a). Since DMA is markedly more potent, Arz could be seen as a DMA pro-drug. Interestingly, in rat liver microsomes, H-DMA was seen to be metabolized efficiently to DMA (Fig. 5), suggesting H-DMA would provide very similar therapeutic opportunities to Arz itself.

Metabolically, the X-DMA SERMs can be categorized into two chemical classes: (Class 1) those that form quinone methides or imines without need for ring-hydroxylation and which can be glucuronidated at the 4'-position (X = OH; NH_2; and Ral); and (Class 2), those for which quinone methide/imine formation is blocked (X = H; F; Br; SO_2Me; OMe/Arz). Theoretically, members of the second class of SERMs can be hydroxylated at the 4'-position. Notably, the 2- and 4-haloestradiols have been reported readily to undergo oxidative defluorination, but not oxidative debromination (Li et al., 1985); although it has been reported that in vivo, oxidative defluorination is not a major metabolic pathway (Stalford et al., 1994).

It is accepted that the oxidative metabolites of tamoxifen and estrogens can be toxic and have the potential to contribute to carcinogenesis (Yager and Liehr, 1996; Dowers et al., 2006), however, oxidative lability contributes to other key factors relevant to drug development, including chemoprevention and bioavailability (Yu et al., 2007). The Class 1 X-DMA SERMs were observed to manifest the expected rich oxidative chemistry, a number of GSH conjugates and metabolites being observed and identified for Ral and DMA. Compatible with calculated oxidation energies, NH_2-DMA was observed to be less labile, but a quinone imine GSH conjugate was identified. Substantial glucuronidation was observed for DMA and Ral, and again NH_2-DMA was less labile, but was 50% glucuronidated in microsomal preperations.

The Class 2 X-DMA SERMs were as expected less susceptible to glucuronidation, each lacking a suitable 4'-substituent. The electron-withdrawing nature of the substituents in F-DMA,

Br-DMA, and $MeSO_2$-DMA was also expected to decrease susceptibility to oxidative bioactivation, as supported by DFT calculations. However, $MeSO_2$-DMA was observed to form a GSH conjugate and more importantly, to be substantially metabolized in rat liver microsomes when studied at lower concentrations. All benzothiophene SERMs can potentially be metabolized to an *o*-quinone, even if diquinone methide formation is blocked, the $MeSO_2$-DMA GSH conjugate was indeed identified as derived from an *o*-quinone. As discussed above, *o*-quinone oxidative metabolites have been implicated in the genotoxicity and carcinogenicity of tamoxifen, endogenous estrogens, and equine estrogens. In contrast, to date, carcinogenicity has not been observed for diquinone methide forming SERMs. It can be postulated that ready oxidation to a diquinone methide may provide an oxidative "safety valve" avoiding *o*-quinone formation and resultant toxicity, albeit at the expense of reduced bioavailability. Testing this postulate will be important for drug discovery of polycyclic aromatic drugs beyond SERMs.

In contrast to $MeSO_2$-DMA, the effect of blocking the 4'-position with an electron withdrawing group in F-DMA and Br-DMA was to give a robust inhibition of oxidative metabolism as observed both by loss of parent SERM and formation of GSH and glucuronide conjugates. The metabolic stability of F-DMA was reflected in vivo after administration to juvenile rats.

The rich oxidative metabolism of most SERM families controls aspects of biological activity, bioavailability, and toxicity. The X-DMA SERMs represent an homologous series for exploring the relationship of structure to activity/reactivity. Herein, the relationship with oxidative metabolism has been quantitatively defined, and shown to be highly responsive to structural tuning of the 4'-substituent, adding to previous correlations of structure with ER-dependent and ER-independent activity (Overk et al., 2007; Qin et al., 2007; Yu et al., 2007).

The use of substituent parameters to explain metabolism and predict bioavailability would represent a powerful tool for further development of benzothiophene SERMs. The simple correlation of in vitro metabolism with redox reactivity was poor, despite reactivity correlating well with electronic substituent parameters. Use of a classical Hansch correlation, adds to simple chemical reactivity the lipophilicity contributions to substrate binding to enzymes and other biomolecules. An excellent coefficient was derived for observed liver microsomal metabolism correlated with a Hansch equation containing 4'-substituent lipophilicity and electronic parameters; this observation is compatible with reported correlations for substrate binding to CYP isoforms. Benzothiophene SERMs are likely to be important clinical therapeutics for the next decade and beyond, therefore understanding of structural correlations is important both for current clinical SERMs and for extension to new therapeutic indications.

References

Barrett-Connor E, Mosca L, Collins P, Geiger MJ, Grady D, Kornitzer M, McNabb MA and Wenger NK (2006) Effects of raloxifene on cardiovascular events and breast cancer in postmenopausal women. *N Engl J Med* **355:**125-137.

Beral V (2003) Breast cancer and hormone-replacement therapy in the Million Women Study. *Lancet* **362:**419-427.

Bolton JL, Trush MA, Penning TM, Dryhurst G and Monks TJ (2000) Role of quinones in toxicology. *Chem. Res. Toxicol.* **13:**135-160.

Burke TW and Walker CL (2003) Arzoxifene as therapy for endometrial cancer. *Gynecol Oncol* **90:**S40-46.

Buzdar A, O'Shaughnessy JA, Booser DJ, Pippen JE, Jr., Jones SE, Munster PN, Peterson P, Melemed AS, Winer E and Hudis C (2003) Phase II, randomized, double-blind study of two dose levels of arzoxifene in patients with locally advanced or metastatic breast cancer. *J. Clin. Oncol.* **21:**1007-1014.

Conzen SD (2003) Current status of selective estrogen receptor medulators (SERMs). *Cancer Journal* **9:**4-11.

Delmas PD, Bjarnason NH, Mitlak BH, Ravoux AC, Shah AS, Huster WJ, Draper M and Christiansen C (1997) Effects of raloxifene on bone mineral density, serum cholesterol concentrations, and uterine endometrium in postmenopausal women. *N. Engl. J. Med.* **337:**1641-1647.

Dowers TS, Qin ZH, Thatcher GR and Bolton JL (2006) Bioactivation of Selective Estrogen Receptor Modulators (SERMs). *Chem Res Toxicol* **19:**1125-1137.

Gao H and Hansch C (1996) QSAR of P450 oxidation: on the value of comparing kcat and km with kcat/km. *Drug Metab Rev* **28:**513-526.

Hansch C, Leo A and Hoekman D (1995) *Exploring QSAR.* ACS, Washington, DC.

Hansch C and Zhang L (1993) Quantitative structure-activity relationships of cytochrome P-450. *Drug Metab Rev* **25:**1-48.

Hochner-Celnikier D (1999) Pharmacokinetics of raloxifene and its clinical application. *Eur. J. Obstet. Gynecol. Reprod. Biol.* **85:**23-29.

Hummel CW, Geiser AG, Bryant HU, Cohen IR, Dally RD, Fong KC, Frank SA, Hinklin R, Jones SA, Lewis G, McCann DJ, Rudmann DG, Shepherd TA, Tian H, Wallace OB, Wang M, Wang Y and Dodge JA (2005) A selective estrogen receptor modulator designed for the treatment of uterine leiomyoma with unique tissue specificity for uterus and ovaries in rats. *J Med Chem* **48:**6772-6775.

Kelminski A (2002) The Study of Tamoxifen and Raloxifene (STAR trial) for the prevention of breast cancer. *Hawaii Med. J.* **61:**209-210.

Kemp DC, Fan PW and Stevens JC (2002) Characterization of raloxifene glucuronidation in vitro: contribution of intestinal metabolism to presystemic clearance. *Drug. Metab. Dispos.* **30:**694-700.

Lewis DF, Jacobs MN and Dickins M (2004) Compound lipophilicity for substrate binding to human P450s in drug metabolism. *Drug Discov Today* **9:**530-537.

Li JJ, Purdy RH, Appelman EH, Klicka JK and Li SA (1985) Catechol formation of fluoro- and bromo-substituted estradiols by hamster liver microsomes. Evidence for dehalogenation. *Mol Pharmacol* **27:**559-565.

Liby K, Rendi M, Suh N, Royce DB, Risingsong R, Williams CR, Lamph W, Labrie F, Krajewski S, Xu X, Kim H, Brown P and Sporn MB (2006) The combination of the rexinoid, LG100268, and a selective estrogen receptor modulator, either arzoxifene or acolbifene, synergizes in the prevention and treatment of mammary tumors in an estrogen receptor-negative model of breast cancer. *Clin Cancer Res* **12:**5902-5909.

Liehr JG (1983) 2-Fluoroestradiol. Separation of estrogenicity from carcinogenicity. *Mol. Pharmacol.* **23:**278-281.

Liehr JG (1984) Modulation of estrogen-induced carcinogenesis by chemical modifications. *Arch. Toxicol.* **55:**119-122.

Liu H, Bolton JL and Thatcher GRJ (2006) Chemical modification modulates estrogenic activity, oxidative reactivity, and metabolic stability in 4'F-DMA, a new benzothiophene selective estrogen receptor modulator. *Chem Res Toxicol* **19:**779-787.

Liu H, Liu J, van Breemen RB, Thatcher GRJ and Bolton JL (2005a) Bioactivation of the selective estrogen receptor modulator desmethylated arzoxifene to quinoids: 4'-fluoro substitution prevents quinoid formation. *Chem Res Toxicol* **18:**162-173.

Liu J, Liu H, van Breemen RB, Thatcher GR and Bolton JL (2005b) Bioactivation of the selective estrogen receptor modulator acolbifene to quinone methides. *Chem. Res. Toxicol.* **18:**174-182.

Overk CR, Peng KW, Asghodom RT, Kastrati I, Lantvit DD, Qin Z, Frasor J, Bolton JL and Thatcher GR (2007) Structure-activity relationships for a family of benzothiophene selective estrogen receptor modulators including raloxifene and arzoxifene. *ChemMedChem* **2:**1520-1526.

Palkowitz AD, Glasebrook AL, Thrasher KJ, Hauser KL, Short LL, Phillips DL, Muehl BS, Sato M, Shetler PK, Cullinan GJ, Pell TR and Bryant HU (1997) Discovery and synthesis of [6-hydroxy-3-[4-[2-(1-piperidinyl)ethoxy]phenoxy]-2-(4-hydroxyphenyl)]b enzo[b]thiophene: a novel, highly potent, selective estrogen receptor modulator. *J Med Chem* **40:**1407-1416.

Qin Z, Kastrati I, Chandrasena RE, Liu H, Yao P, Petukhov PA, Bolton JL and Thatcher GRJ (2007) Benzothiophene selective estrogen receptor modulators with modulated oxidative activity and receptor affinity. *J Med Chem* **50:**2682-2692.

Rossouw JE, Anderson GL, Prentice RL, LaCroix AZ, Kooperberg C, Stefanick ML, Jackson RD, Beresford SA, Howard BV, Johnson KC, Kotchen JM and Ockene J (2002) Risks and benefits of estrogen plus progestin in healthy postmenopausal women: principal results From the Women's Health Initiative randomized controlled trial. *Jama* **288:**321-333.

Sarver JG, White D, Erhardt P and Bachmann K (1997) Estimating xenobiotic half-lives in humans from rat data: influence of log P. *Environ Health Perspect* **105:**1204-1209.

Sato M, Turner CH, Wang T, Adrian MD, Rowley E and Bryant HU (1998) LY353381.HCl: a novel raloxifene analog with improved SERM potency and efficacy in vivo. *J. Pharmacol. Exp. Ther.* **287:**1-7.

Shibutani S, Ravindernath A, Suzuki N, Terashima I, Sugarman SM, Grollman AP and Pearl ML (2000) Identification of tamoxifen-DNA adducts in the endometrium of women treated with tamoxifen. *Carcinogenesis* **21:**1461-1467.

Snyder KR, Sparano N and Malinowski JM (2000) Raloxifene hydrochloride. *Am. J. Health Syst. Pharm.* **57:**1669-1675; quiz 1676-1668.

Stalford AC, Maggs JL, Gilchrist TL and Park BK (1994) Catecholestrogens as mediators of carcinogenesis: correlation of aromatic hydroxylation of estradiol and its fluorinated analogs with tumor induction in Syrian hamsters. *Mol Pharmacol* **45:**1268-1272.

Suh N, Glasebrook AL, Palkowitz AD, Bryant HU, Burris LL, Starling JJ, Pearce HL, Williams C, Peer C, Wang Y and Sporn MB (2001) Arzoxifene, a new selective estrogen receptor modulator for chemoprevention of experimental breast cancer. *Cancer Res* **61:**8412-8415.

van Leeuwen FE, Benraadt J, Coebergh JW, Kiemeney LA, Gimbrere CH, Otter R, Schouten LJ, Damhuis RA, Bontenbal M, Diepenhorst FW and et al. (1994) Risk of endometrial cancer after tamoxifen treatment of breast cancer. *Lancet* **343:**448-452.

Vogel VG, Costantino JP, Wickerham DL, Cronin WM, Cecchini RS, Atkins JN, Bevers TB, Fehrenbacher L, Pajon ER, Jr., Wade JL, 3rd, Robidoux A, Margolese RG, James J, Lippman SM, Runowicz CD, Ganz PA, Reis SE, McCaskill-Stevens W, Ford LG, Jordan VC and Wolmark N (2006) Effects of tamoxifen vs raloxifene on the risk of developing invasive breast cancer and other disease outcomes: the NSABP Study of Tamoxifen and Raloxifene (STAR) P-2 trial. *Jama* **295:**2727-2741.

Yager JD and Liehr JG (1996) Molecular mechanisms of estrogen carcinogenesis. *Annu Rev Pharmacol Toxicol* **36:**203-232.

Yu B, Dietz BM, Dunlap T, Kastrati I, Lantvit DD, Overk CR, Yao P, Qin Z, Bolton JL and Thatcher GR (2007) Structural modulation of reactivity/activity in design of improved benzothiophene selective estrogen receptor modulators: induction of chemopreventive mechanisms. *Mol Cancer Ther* **6:**2418-2428.

Yu L, Liu H, Li W, Zhang F, Luckie C, van Breemen RB, Thatcher GR and Bolton JL (2004) Oxidation of raloxifene to quinoids: potential toxic pathways via a diquinone methide and o-quinones. *Chem. Res. Toxicol.* **17:**879-888.

Footnotes:

This work is supported by NIH Grants CA102590 and CA79870.

Greg Thatcher, Dept. of Medicinal Chemistry & Pharmacognosy, College of Pharmacy, University of Illinois at Chicago, 833 S Wood St., Chicago, IL 60612; Tel: 312-355-5282; E-mail: thatcher@uic.edu

Figure Legends

Figure 1. Structures of clinical and preclinical SERMs; structures of benzothiophene SERMs, including X-DMA SERMs; structures of previously identified GSH conjugates of DMA.

Figure 2. (A) Calculated BDE for one and two electron oxidations of benzothiophenes in formation of semiquinone radicals, a diquinone methide, and a quinone imine. **(B)** Substituent effects for benzothiophene derivatives on OH bond homolysis: a) σ_p vs ΔG ($\rho = 1.89$, $r^2 = 0.97$); b) σ_p vs BDE ($\rho = 2.01$, $r^2 = 0.97$); c) σ_p^+ vs ΔG ($r^2 = 0.93$); d) σ_p^+ vs BDE ($r^2 = 0.93$).

Figure 3. Representative chromatograms of incubations of benzothiophene SERMs (Ral, DMA, NH2-DMA, and MeSO2-DMA; 10 μM) with induced rat liver microsomes (1 mg/ml) in the presence of NADPH (1 mM) and GSH (500 μM) for 30 min. Detection of metabolites and conjugates was by UV-Vis absorbance (shown in arbitrary units) at 316 nm and all annotated peaks were characterized by LC-MS-MS analysis.

Figure 4. **(A**) MS-MS spectrum of NH2-DMA quinone imine GSH conjugate formed from nucleophilic substitution at the 3-position. **(B)** MS-MS spectra of N-dealkylated metabolites of NH2-DMA and DMA. **(C)** MS-MS spectrum of $MeSO_2$-DMA GSH conjugate.

Figure 5. Representative chromatograms of incubations of benzothiophene SERMs (H-DMA, arzoxifene, F-DMA, and Br-DMA; 10 μM) with induced rat liver microsomes (1 mg/ml) in the presence of NADPH (1 mM) and GSH (500 μM) for 30 min. Detection of metabolites and conjugates was by UV-Vis absorbance at 316 nm and all annotated peaks were characterized by

LC-MS-MS analysis. GSH conjugates of H-DMA, F-DMA, Br-DMA were not detected by LC-MS-MS.

Figure 6. **(A)** Plot of remaining parent benzothiophene SERM (1 μM) after incubation with induced rat liver microsomes (0.5 mg/ml) in the presence of NADPH (1 μM) for 30 min. Detection of metabolites and conjugates was by UV-Vis absorbance at 316 nm and all annotated peaks were characterized by LC-MS-MS analysis. **(B)** Plot of glucuronide conjugate formation from benzothiophene SERMs (30 μM) in incubations of either human intestinal microsomes or human liver microsomes (0.5 mg.ml) with UDPGA (1 mM) and alamethicin (50 μg/ml).

Figure 7. Correlations of X-DMA SERM metabolism using molecular and substituent parameters, or computed scores. Depletion of parent X-DMA SERMs in rat liver microsomes correlated (A) against ClogP and (B) in a Hansch correlation using substituent parameters. (C) Correlation of glucuronide formation with depletion of parent SERMs showing SERMs susceptible to 4'-substituent conjugation as outliers. (D) Computed VolSurf PSA scores for CYP3A4 metabolic susceptibility correlated with observed metabolic stability in rat liver microsomes: solid squares and line PSA1 score; open squares and dashed line PSA2 score.

Figure 8. Concentration of parent X-DMA SERMs remaining in blood plasma collected from rats after in vivo drug administration over 3 days either with or without co-administration of estradiol (E_2) as the benzoate. The concentration was measured using quantitative LC-MS on the blood plasma (60 μL) using authentic samples of SERMs in untreated plasma to derive a standard curve. N=5; ** p-value < 0.001.

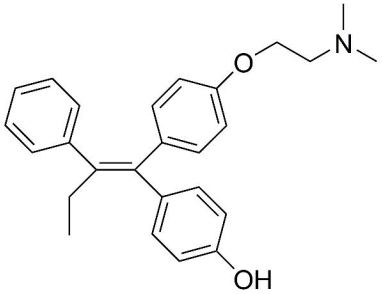

4-hydroxytamoxifen

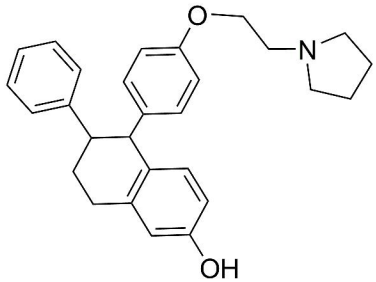

lasofoxifene

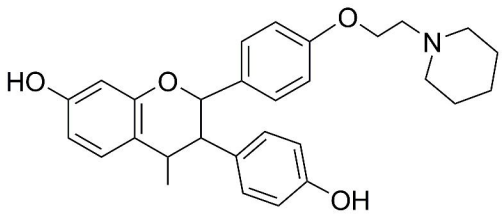

acolbifene

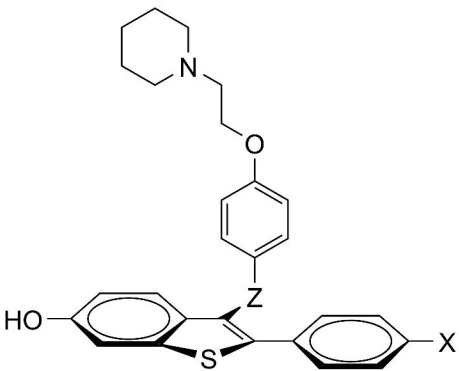

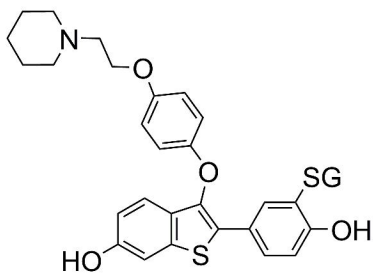

DMA-SG1

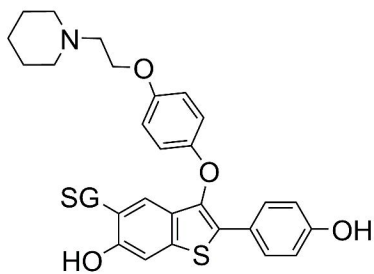

DMA-SG2

Raloxifene	Z = CO; X = OH		
Arzoxifene	Z = O; X = OMe	ClogP	7.5
DMA	Z = O; X=OH		6.9
H-DMA	Z = O; X=H		7.5
F-DMA	Z = O; X=F		7.7
Br-DMA	Z = O; X=Br		8.4
NH_2-DMA	Z = O; X= NH_2		6.4
SO_2Me-DMA	Z = O; X= SO_2Me		5.9

Figure 1

Figure 2

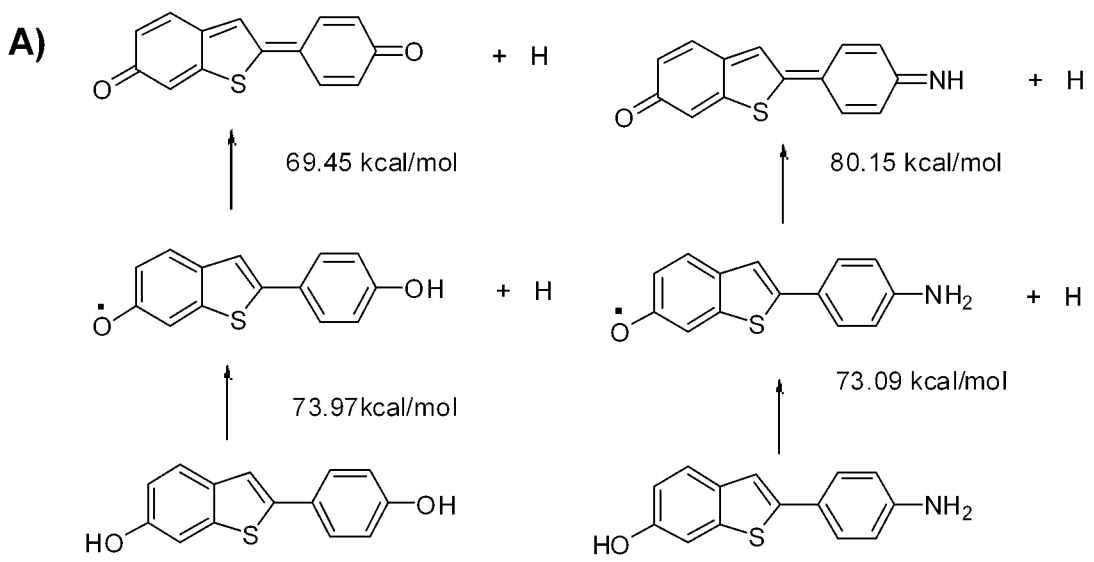
A)
O
O
S
+ H
69.45 kcal/mol
OH
+ H
73.97kcal/mol
HO
OH
NH
+ H
80.15 kcal/mol
NH2
+ H
73.09 kcal/mol
HO
NH2

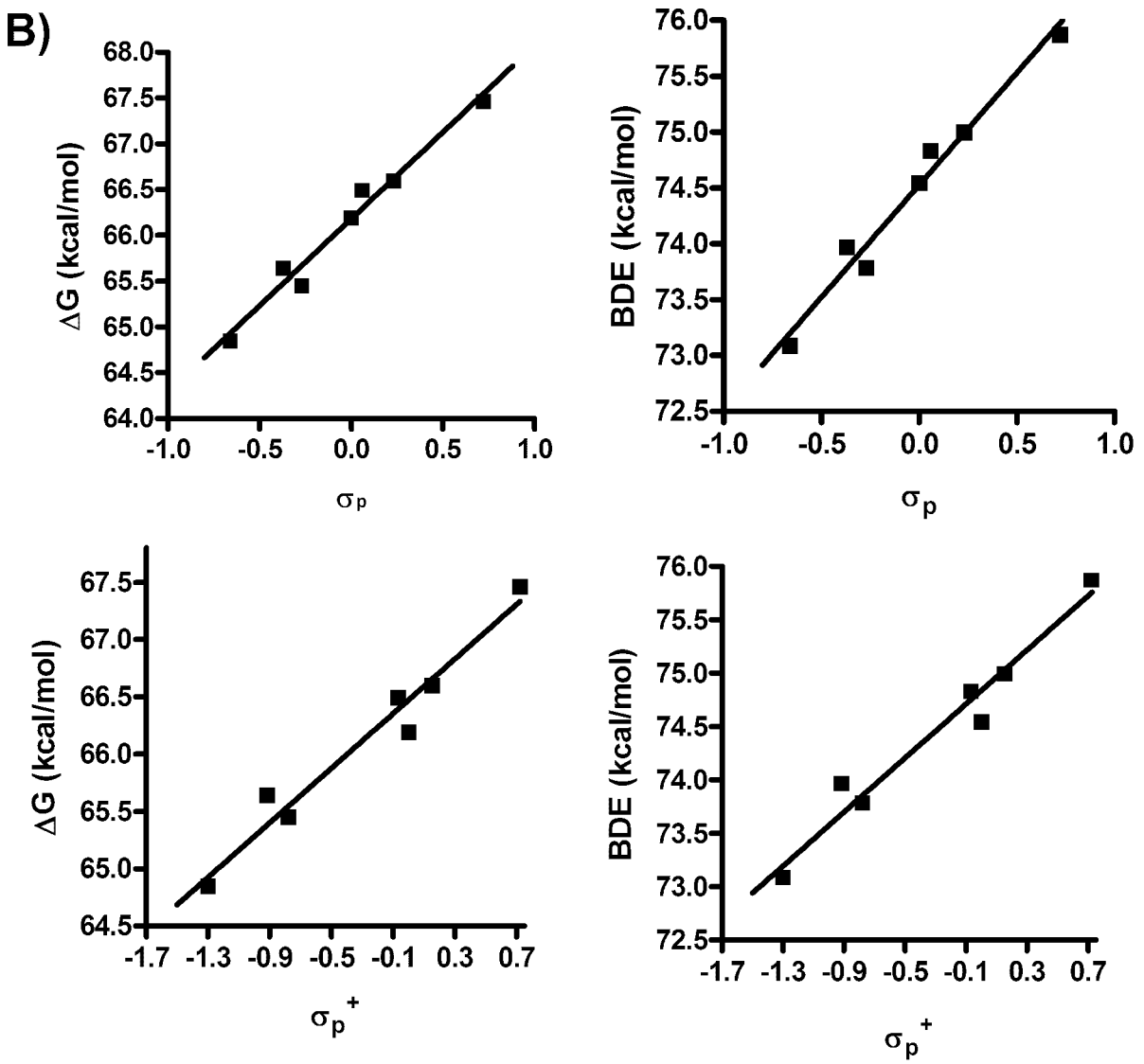
B)
ΔG (kcal/mol)
68.0
67.5
67.0
66.5
66.0
65.5
65.0
64.5
64.0
-1.0
-0.5
0.0
0.5
1.0
σp
BDE (kcal/mol)
76.0
75.5
75.0
74.5
74.0
73.5
73.0
72.5
-1.0
-0.5
0.0
0.5
1.0
σp
ΔG (kcal/mol)
67.5
67.0
66.5
66.0
65.5
65.0
64.5
-1.7
-1.3
-0.9
-0.5
-0.1
0.3
0.7
σp+
BDE (kcal/mol)
76.0
75.5
75.0
74.5
74.0
73.5
73.0
72.5
-1.7
-1.3
-0.9
-0.5
-0.1
0.3
0.7
σp+

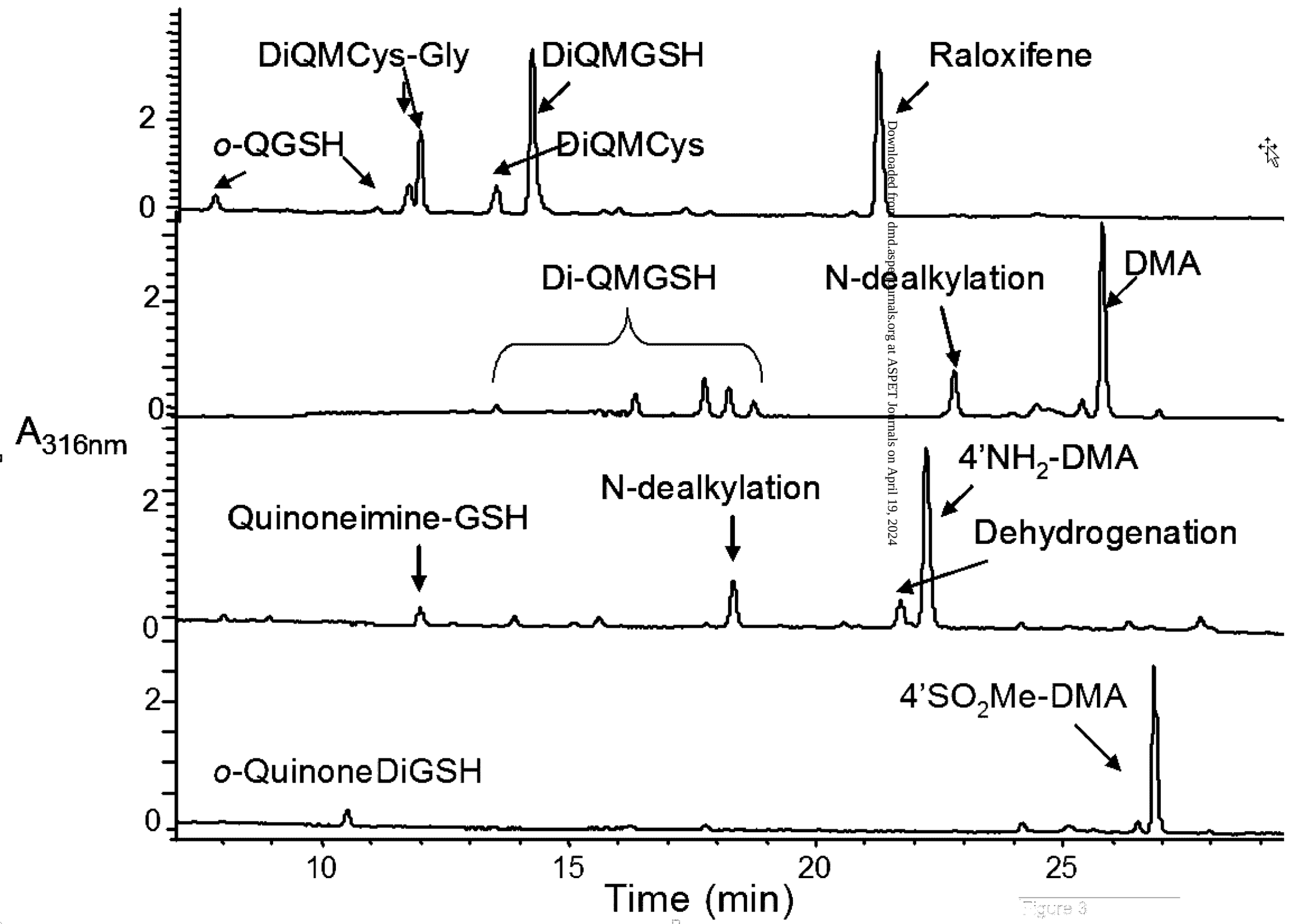

Figure 3

DMD Fast Forward. Published on October 20, 2008 as DOI: 10.1124/dmd.108.023408
This article has not been copyedited and formatted. The final version may differ from this version.

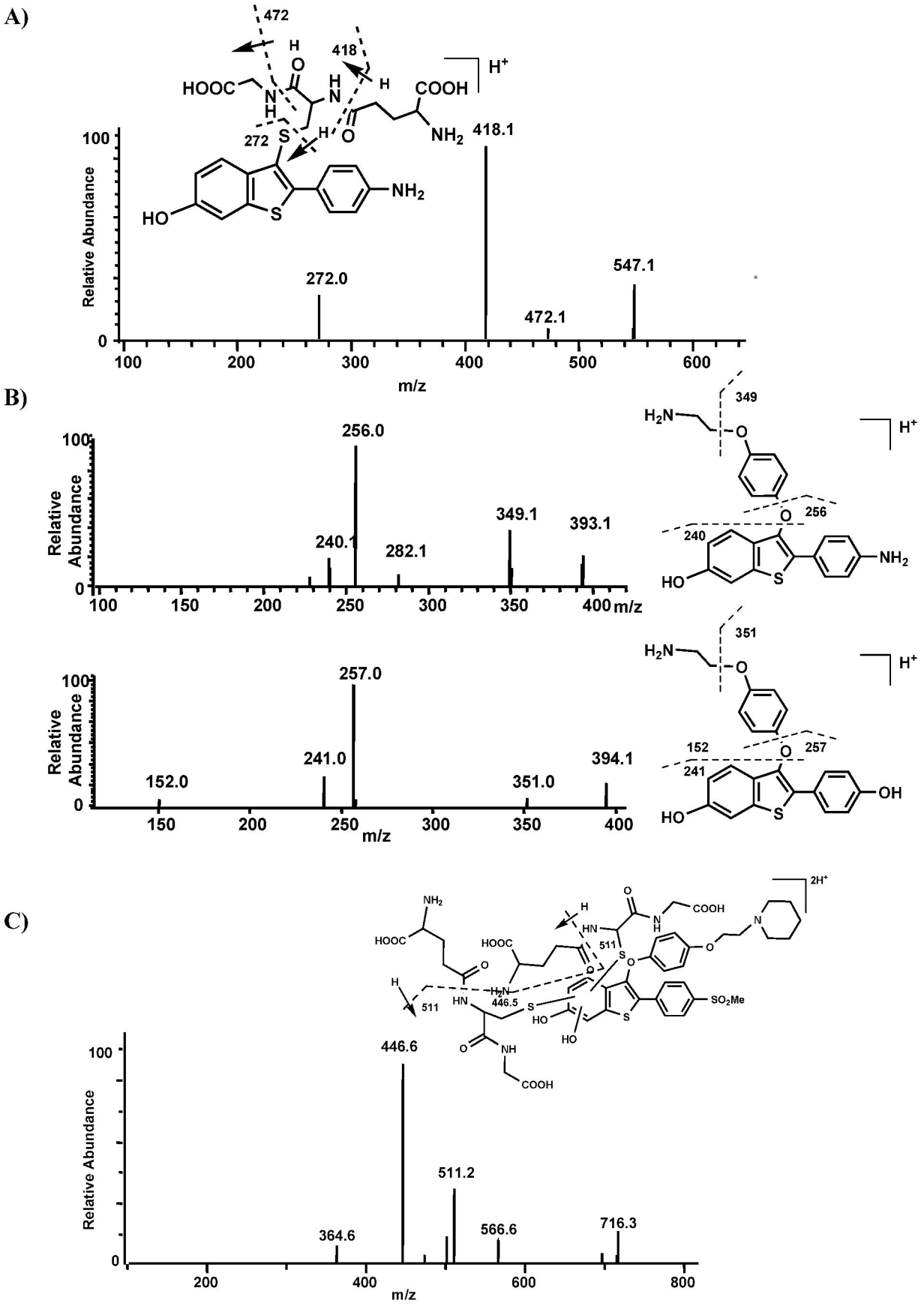

Figure 4

DMD Fast Forward. Published on October 20, 2008 as DOI: 10.1124/dmd.108.023408
This article has not been copyedited and formatted. The final version may differ from this version.

Figure 5

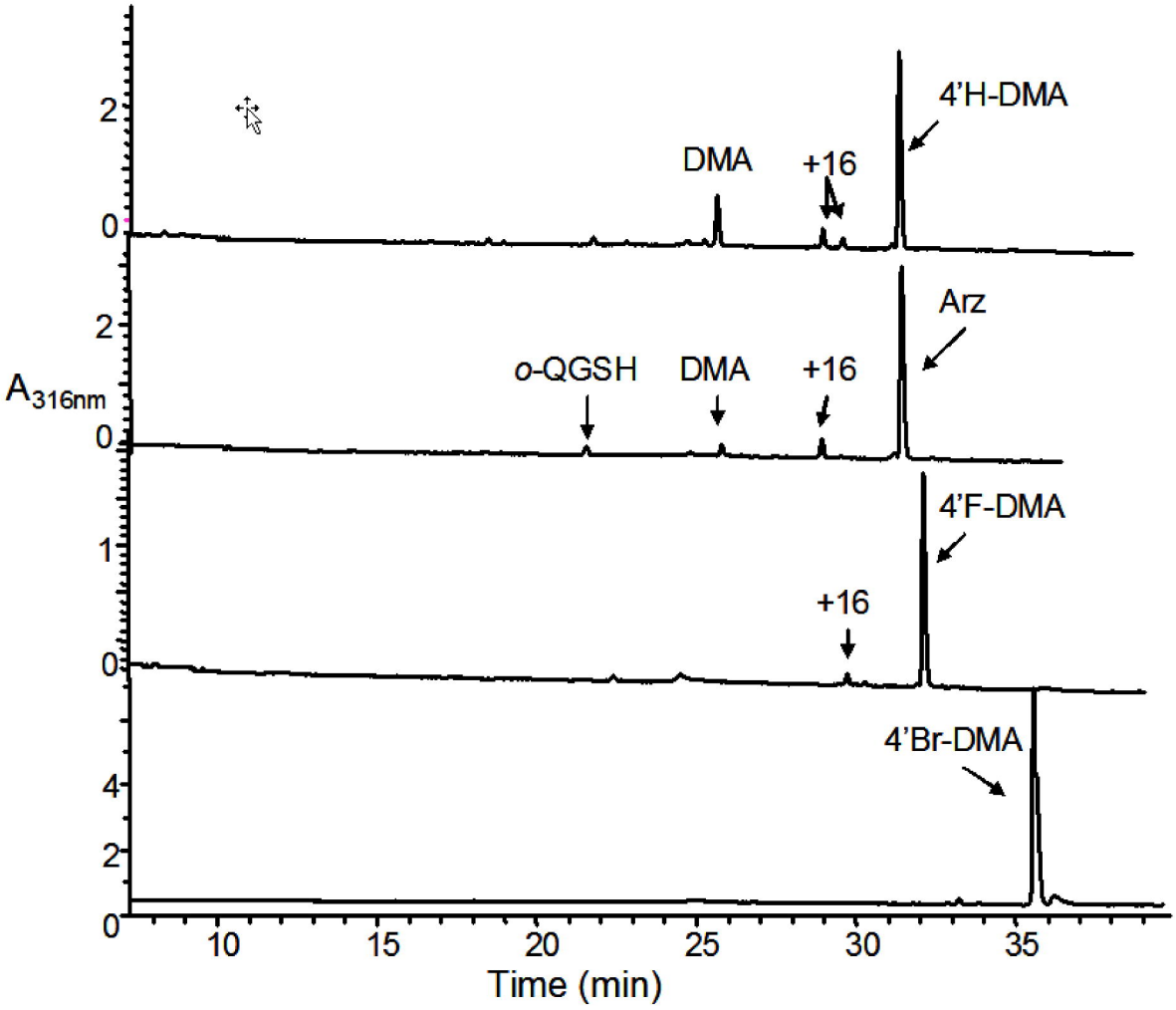

Figure 6

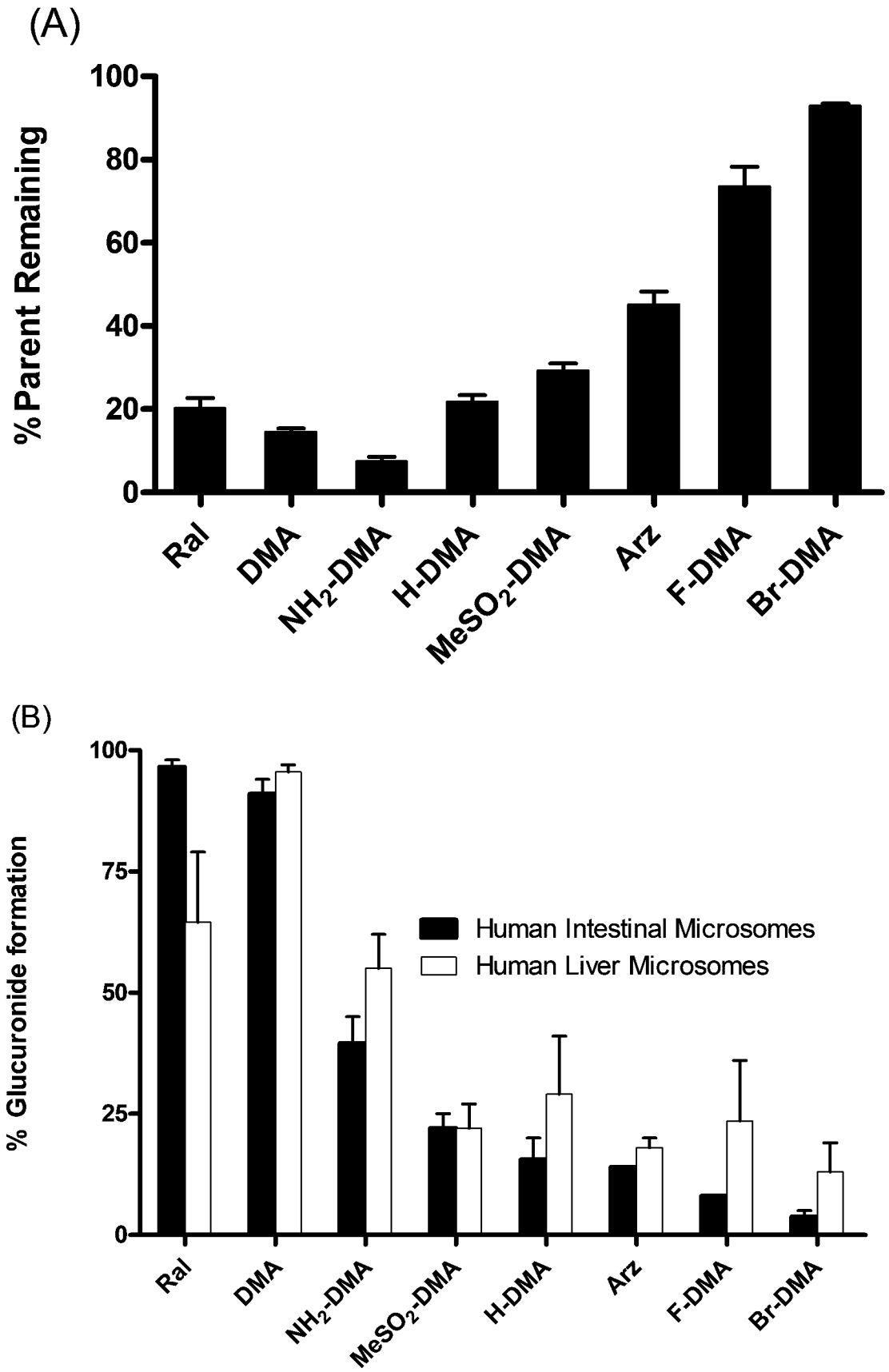
(A)
% Parent Remaining
100
80
60
40
20
0
Ral
DMA
NH2-DMA
H-DMA
MeSO2-DMA
Arz
F-DMA
Br-DMA
(B)
% Glucuronide formation
100
75
50
25
0
Human Intestinal Microsomes
Human Liver Microsomes
Ral
DMA
NH2-DMA
MeSO2-DMA
H-DMA
Arz
F-DMA
Br-DMA

Figure 7

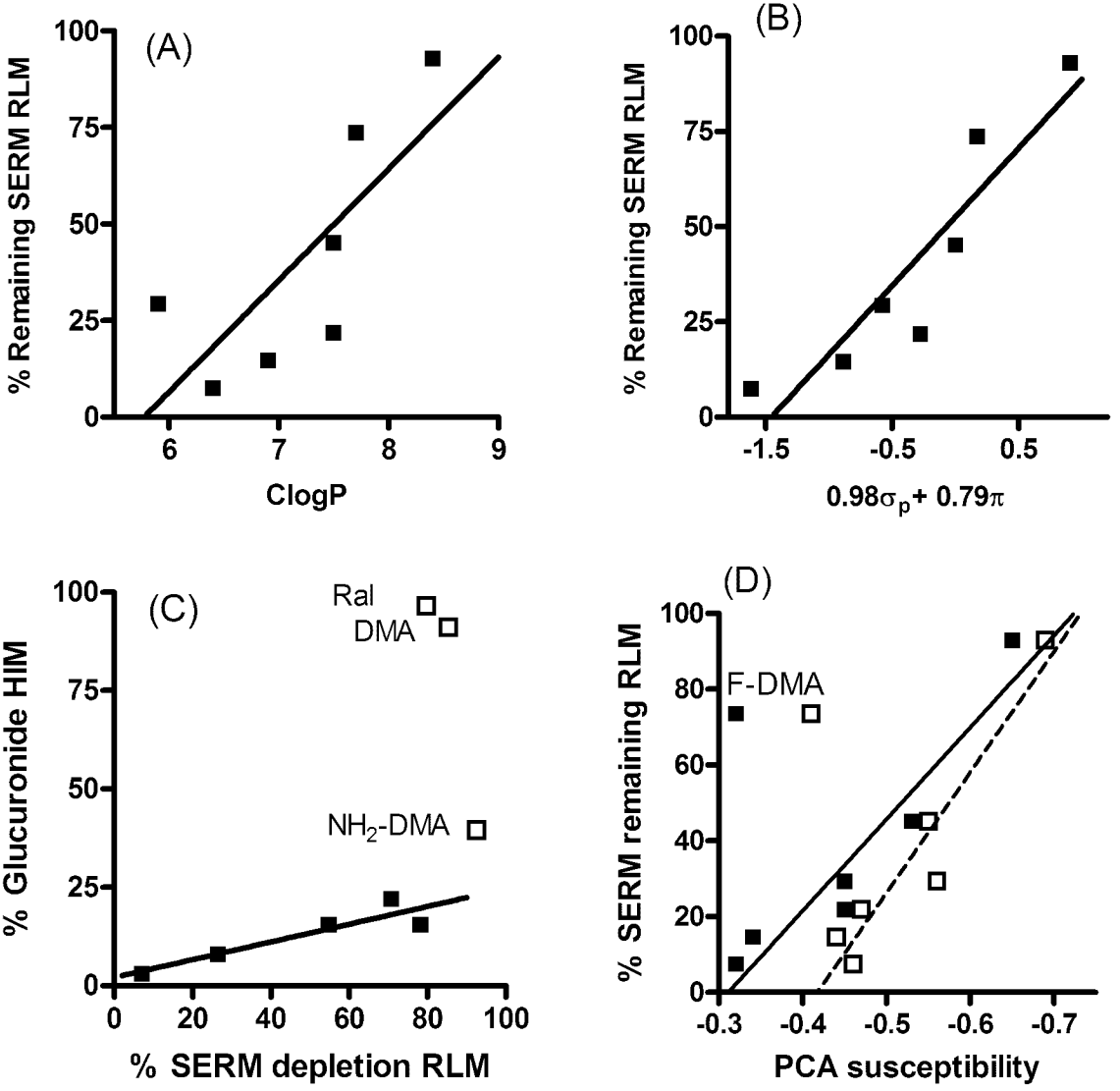
(A)
% Remaining SERM RLM
100
75
50
25
0
6
7
8
9
ClogP
(B)
% Remaining SERM RLM
100
75
50
25
0
-1.5
-0.5
0.5
0.98σp+ 0.79π
(C)
Ral
DMA
NH2-DMA
% Glucuronide HIM
100
75
50
25
0
0
20
40
60
80
100
% SERM depletion RLM
(D)
F-DMA
% SERM remaining RLM
100
80
60
40
20
0
-0.3
-0.4
-0.5
-0.6
-0.7
PCA susceptibility

DMD Fast Forward. Published on October 20, 2008 as DOI: 10.1124/dmd.108.023408
This article has not been copyedited and formatted. The final version may differ from this version.

Figure 8